Proceedings of ICRC 2001: 1210 © Copernicus Gesellschaft 2001

ICRC 2001

Characteristics of upward-going EeV tau neutrino airshowers.

D. B. Kieda

Department of Physics, University of Utah, Salt Lake City, UT 84114, U.S.A.

Abstract. We calculate the properties of the Cerenkov light emitted by upward-going extensive air showers (EAS) through Monte Carlo Simulation. Cerenkov light spectrum, lateral distribution, and arrival time distributions are calculated for a wide range of energies, zenith angles and atmospheric conditions, assuming observation by a satellite with a 100 km orbital height. The resulting simulations indicate that it may be feasible to detect upward-going tau neutrino showers from space with a fairly large aperture (100 km^2 sr) for energies above 10 PeV.

1 Introduction

Recent observations of cosmic rays with energies beyond the GZK cutoff (Bird et al. , 1993; Hayashida et al. , 1994) have sparked considerable theoretical interest in the possible sources of these particles. Sources such as decay of topological defects (Sigl et al. , 1999, 1995), Gamma ray Bursts (Waxman and Bachall , 1997; Vietri , 1997), Active Galactic Nuclei (Biermann , 1998; Yoshida et al. , 1998) not only produce super-GZK hadrons and leptons, but can also produce large fluxes of Ultra-High energy neutrinos. In addition, interactions of the super-GZK cosmic rays with the 3° K cosmic microwave background radiation can also produce a flux of Ultra-High energy neutrinos.

The existence of muon neutrino flavor-changing oscillations to tau neutrinos, which are evidenced by measurements of atmospheric neutrino fluxes, can provide a novel detection mechanism at Ultra-High energies. At energies above 10^{17} eV, the Earth is opaque to through going neutrinos. However, due to lepton number conserving neutrino oscillations, tau neutrinos can regenerate to allow propagation through the Earth. One may therefore be able to detect these neutrinos by looking for Cerenkov light emitted by 'upward-going' EAS initiated by the particles interacting at the crust of the earth's surface (Cline and Stecker, 2000).

Correspondence to: D. B. Kieda (kieda@physics.utah.edu)

Cerenkov light emitted by an upward-going EAS will have distinct features compared to the traditional downward-going EAS. In the simplest approximation, the Cerenkov light will be geometrically spread to a larger lateral distance scale as one will observe the upward-going light at a typical orbital distance (100 km or more), compared to a downward-going distance of 10 km or less. One could naively achieve an approximation of the upward-going Cerenkov light characteristics simply by expanding the downward-going Cerenkov light pool by this geometric factor.

However, this simple extrapolation is inaccurate for several reasons. The Cerenkov angle progresses from large to small as the EAS develops, exactly the opposite from the downward-going case. Secondary particle decay will be suppressed due to the high density of the atmosphere; unstable π/K's which usually could travel a long distance/time without interacting will not be afforded this possibility in the dense lower atmosphere. The upward-going Cerenkov light may also be affected by atmospheric conditions which do not affect downward-going distributions; high cirrus clouds (above 15-20 km) is one example. Consequently, simple extrapolations of downward-going Cerenkov distributions will not provide an accurate representation of the upward-going Cerenkov signature.

In this paper, we describe the calculated results of Monte Carlo simulated distributions of Cerenkov radiation emitted by upward-going particles. In this conference report, initial results from pure electromagnetic showers induced by upward-going electrons will be presented. These results demonstrate the general characteristics of the Cerenkov light from upward-going EAS. They will not be strongly influenced by the π/K interaction density effects described above, which, combined with the hadronic interaction transverse momenta, can provide increased angular distributions of the Cerenkov photons over what is presented in this paper. At the ICRC, the talk will include distributions calculated for upward-going tau neutrinos, which will be more strongly affected by these density effects.

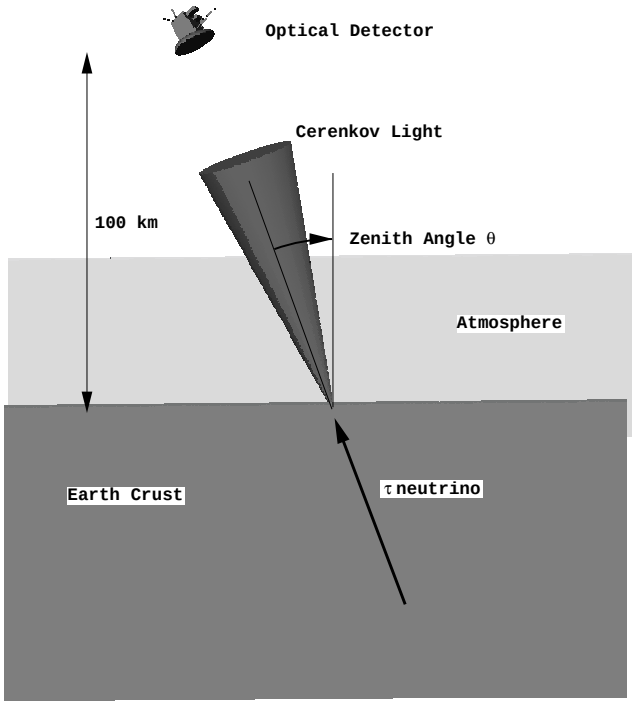

Fig. 1. Shower simulation geometry for calculation of Cerenkov light from Upward-going Tau-induced EAS.

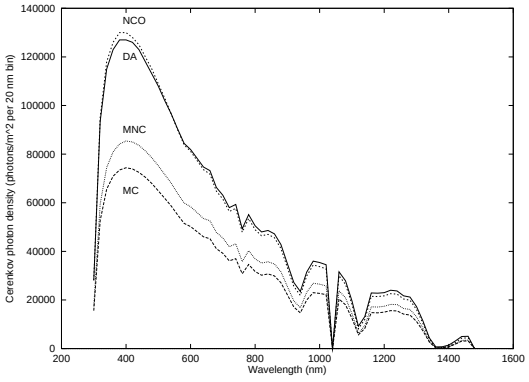

Fig. 2. Cerenkov Light spectral distribution for upward-going 10 EeV electron with 45° zenith angle trajectory observed at 100 km height. Atmospheric models labels are: DA: Desert Aerosol; NCO:Naval model, with Cirrus clouds, Openocean; MC: Marine with Cirrus clouds; MNC: Marine with No Cirrus. Spectrum is measured at 1.1 km from shower axis. Horizontal Axis: Photon Wavelength (nm). Vertical Axis: Cerenkov Photon density (photons/m^2 per 20 nm bin.)

2 Simulation Description

2.1 Simulation Geometry

Figure 1 illustrates the geometry used in the EAS simulation. All simulations are done by placing the upward-going primary particle (in this case, an electron) at sea level and then propagating the particle upward through the atmosphere with standard EAS simulation code. All calculations are done in the 'flat-earth' approximation; this will result in significant errors for shower trajectories with zenith angles well beyond 60°.

2.2 Extensive Air Shower Simulation

The simulation used in this calculation is based upon the MOCCA simulation code (Hillas , 1982,b) modified to include spectral information,spectral dependent atmospheric light propagation, (Kieda , 1995) as well as custom modifications to allow upward propagation of light and particles. All showers were run using the MOCCA thinning procedure, with showers thinned when the secondary energy reached 10^{-4} of the primary energy. Photodetector spectral response is not included in these calculations.

2.3 Atmospheric Model

Four atmospheric optical transmission models were used for the simulations. These models are derived form standard LOWTRAN7 simulations(Kneizys et al. , 1988), and include a wind-driven desert aerosol model, a maritime model with no cirrus clouds, a maritime model with high cirrus clouds, and a standard 'navy' open-ocean model with high cirrus clouds. These models provide typical representations of the ranges of atmospheric transmission that are to be expected over the majority of observing conditions. For each model, optical attenuation curves were calculated as a function of wavelength, zenith angle of the trajectory, and integrated distance from the Cerenkov emission region to the optical receiver located in a 100 km orbit above the ground. In practice, the integrated optical attenuation does not change significantly once the optical receiver is above 50 km, as one is above 99.9% of the atmosphere at this height.

3 Cerenkov Light Characteristics

3.1 Spectral Characteristics

Figure 2 illustrates the spectral distribution of the Cerenkov light for an upward-going 10 EeV electron with a 45° zenith angle. The optical spectrum peaks at 400-450 nm, substantially longer than the usual peak cerenkov wavelength (usually around 330-350 nm). Substantially more photons exist between 400-600 nm than from 200-400 nm. Consequently, the optimal observation wavelength may be substantially longer than that which is used for Nitrogen Fluorescence detectors like OWL and Fly's Eye (about 350 nm). Factors of 2 in the photon density are evident, especially near the peak wavelength, for different atmospheric observing conditions.

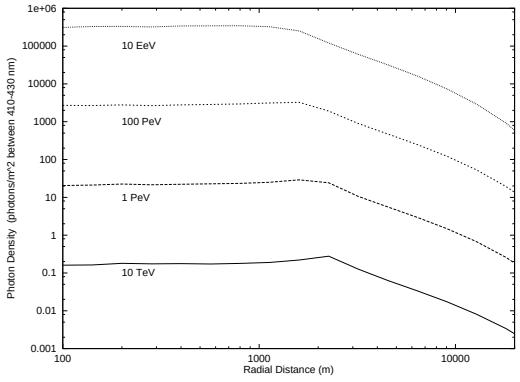

Fig. 3. Cerenkov Light lateral distribution for upward-going electrons of various primary energies observed at 100 km height. Atmospheric model is Navy Cirrus Open ocean. Shower trajectory is vertical ($\theta = 0^{\circ}$). Horizontal Axis: radial distance (meters). Vertical Axis: Cerenkov Photon density (photons/m^2 in spectral window between 410-430 nm.)

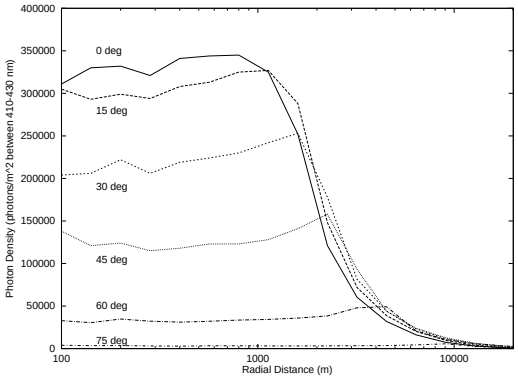

Fig. 4. Cerenkov Light lateral distribution for upward-going 10 EeV electron with different zenith angle trajectories observed at 100 km height. Atmospheric model is Navy Cirrus Open ocean. Horizontal Axis: radial distance (meters). Vertical Axis: Cerenkov Photon density (photons/m^2 in spectral window between 410-430 nm.)

3.2 Lateral Distribution

Figure 3 illustrates the lateral distribution of the Cerenkov light, observed in the spectral window between 410-430 nm for a vertical trajectory upward-going electron. The distribution is flat out to distances of 1-2 km, and changes into a power law dependence of R^{-2} beyond a characteristic cutoff radius. The photon yield scales well with the primary energy, but the cutoff radius is energy dependent, moving to smaller radii at higher energies. The energy dependence of the cutoff radius is due to the inverse propagation of the EAS; at higher energies, a larger fraction of the air shower penetrates higher into the atmosphere, where the Cerenkov emission angle is reduced. The photons emitted by the EAS in the less dense atmosphere are also closer to the detector, reducing the geometrical spread of the cerenkov photons. Consequently, these photons will increasingly contribute to smaller radii as one increases primary energy, thereby pushing the cutoff radius to smaller values with increasing energy. An approximate expression which fits the energy dependence of the cutoff radius R_c is $R_c = 4600 - 75 \times \ln(E)$ meters where the primary energy E is given in eV.

Figure 4 illustrates the variation of the Cerenkov light lateral distribution as a function of the zenith angle. As one goes to large zenith angles, the lateral distribution continues to grow geometrically with the increasing pathlength to the detector. The 'bump' in the lateral distribution just at the cutoff radius is consistent with the lateral distance calculated by combining the Cerenkov light emission angle at ground level with the pathlength distance to the detector.

3.3 Angular Distribution

Figure 5 illustrates the angular spread of the Cerenkov light with respect to the primary electron direction, as measured in the shower-detector plane, which is defined as the plane containing both the measured Cerenkov photon direction vector as well as the vector of shortest distance from the detector to the EAS axis. The locally observed Cerenkov photons do not point back to the direction of the original shower, but instead are offset from this direction by a few degrees or more. The offset and spread is dependent upon the lateral distance to the EAS shower axis, and is related to the geometrical relationship between the viewing angle of the shower and the longitudinal and lateral spread of the Cerenkov light emitted by the shower. Following techniques developed for monocular reconstruction of TeV γ-rays with ground-based Cerenkov detectors, this spread of the Cerenkov light can be used to estimate the distance to the shower axis. This distance is essential for the determination of the primary energy of the particle initiating the EAS.

3.4 Time Distribution

Figure 6 illustrates the arrival time delay and time spread of the Cerenkov photons as a function of the lateral radial observation distance for different zenith angle trajectories of an upward-going electron. At very large observation distances, the time spread is large, while the photon flux drops rapidly with increasing radial distance (Figure 3). The combination of these two effects will limit the maximum radius to which one can observe a EAS at a given energy when the EAS is observed against background light due to terrestrial and backscattered lunar, solar, and astrophysical light.

4 Discussion

The OWL observatory (Scarsi et al. , 1999) provides a typical example of an optical observatory that might possess sensitivity to upward-going Cerenkov events generated by tau neutrinos. OWL is expected to have an optical collection area on the order of about 5 m^2, an orbital height of about

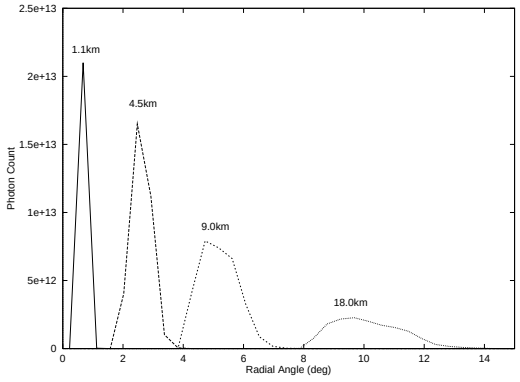

Fig. 5. Cerenkov Light angular distribution in the plane of the observed Cerenkov light for upward-going EAS initiated by electron with 0○ zenith angle trajectory observed at 100 km height. Atmospheric model is Navy Cirrus Open ocean. Horizontal Axis: Angle of the Cerenkov light arrival direction with respect to to the primary electron direction in the plane containing the shower image (degrees). Vertical Axis: Total photon count observed in annulus at various radial bins (unnormalized, but corrected for solid angle).

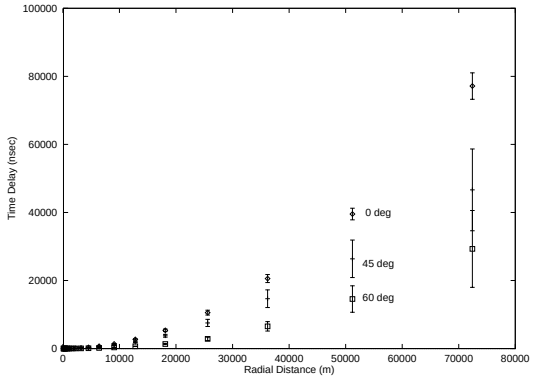

Fig. 6. Cerenkov Light arrival time for upward-going 10 EeV electron with different zenith angle trajectories observed at 100 km height. Atmospheric model is Navy Cirrus Open ocean. Horizontal Axis: radial distance (meters). Vertical Axis: Time delay with respect to arrival of first photons (nsec).

500 km, and an Earth observing background of about 100 photons $m^{-2}nsec^{-1}sr^{-1}$. Since this distance is a factor of 5 larger than that used in these calculations, the Cerenkov light pool will geometrically spread itself out by an additional factor of 5 , and the Cerenkov light density will be suppressed by a factor of 25.

If we try to observe the shower at a distance of 10 km, the typical time spread of the photons is on the order of 100 nsec, implying a DC background intensity of 5×10^4 photons sr^{-1}. The typical cerenkov light pulse is spread out in angular space at this distance (extrapolated to 500km from Figure 5) is a cigar shaped image subtending 1 degree by less than 0.2 degrees, or therefore subtending a solid angle of about 5×10^{-5} sr. Consequently, the background fluctuation noise in the entire Cerenkov image observed at 10 km lateral distance is about 2 photons.

Using the lateral distribution curve of Figure 3, extrapolated by a factor of 5 in observing distance, and using the poorer atmospheric transmission (MC), one estimates an approximate energy threshold of around 10 PeV. The uncertanty of the night sky background level results in roughly a factor 2 uncertainty in this threshold estimate. The energy threshold is likely to be somewhat higher since we have assumed 100% optical collection efficiency. The effective detection aperture for such neutrinos would be on the order of 100 km^2 sr at 10 PeV. To increase the detection aperture, one could observe the showers at larger zenith angles, but one will have to pay a commensurate penalty in the energy threshold as the Cerenkov light pool will become substantially less dense.

We note that this energy threshold is substantially higher and the detection aperture is substantially smaller than estimated by others(Cline and Stecker, 2000).

5 Summary

We have simulated the characteristics of Cerenkov light emitted by upward-going EAS induced by electrons. These simulations provide the first approximation to light yields expected from EAS generated by upward-going tau neutrinos interacting in the Earth's crust. Initial estimates suggest an energy threshold for observation of at least 10 PeV at a lateral distance of 10 km from the shower, assuming a 500 km orbital observation distance. Future work, to be presented at the conference, will include simulation of the tau-induced upward-going EAS as well as the production of the tau from the tau neutrino. It has been suggested that this process may yield a unique shower development signature that may be used to uniquely identify the tau neutrino primary(Cline and Stecker, 2000).

Acknowledgements. The author acknowledges useful discussions with P. Sokolsky and V. Vassiliev. This work was supported under NSF Grant # PHY 0079704

References

Biermann,P.L. , AIP CP 433, 22, 1998.
Bird, D. et al. , Phys. Rev. Lett. 71, 4301, 1993.
Cline, D. B. and Stecker, F. W., UCLA Workshop on High Energy Neutrino Astrophysics, astro-ph/0003459, 2000.
Hayashida, N. et al. , Phys. Rev. Lett. 73, 3491, 1994.
Hillas, M. A. , J. Phys. G: Nucl. Phys. 8, 1461, 1982.
Hillas, M. A. , J. Phys. G: Nucl. Phys. 8, 1475, 1982.
Kieda, D. B. , Astropart. Phys. 4, 133, 1995.
Kneizys, F.X. et al. , User's Guide to LOWTRAN7, Air Force Geophysics Laboratory Publication AFGL-TR-88-0177, 1988.
Scarsi, l. et al. , Proc. 26^{th} ICRC, Salt Lake City 2, 384, 1999.
Sigl, G. et al. , Phys. Rev. D 59, 43504, 1999.
Sigl, G. et al. , Science, 270, 1977, 1995.
Vietri, M. , Phys. Rev. Lett. 78, 4328, 1997.
Waxman, E. and Bachall, J., Phys. Rev. Lett. 78, 2293, 1997.
Yoshida, S. et al. , Phys. Rev. Lett. 81, 5505, 1998.